Springer

KSME

Journal of Mechanical Science and Technology 24 (6) (2010) 1353~1362
www.springerlink.com/content/1738-494x
DOI 10.1007/s12206-010-0341-4

Design and analysis of an active steering bogie for urban trains †

Joon-Hyuk Park*, Hyo-In Koh, Hyun-Moo Hur, Min-Soo Kim and Won-Hee You

Korea Railroad Research Institute, Uiwang-si, Gyeonggi-do, 437-757, Korea

(Manuscript Received June 9, 2009; Revised December 28, 2009; Accepted March 10, 2010)

Abstract

The conventional railway vehicle was designed to ensure running stability using high stiffness elements for primary suspensions. Curving performance of the railway vehicle is relatively low because the natural steering motion of a wheelset is constrained by the high stiffness suspensions. High running stability has always been in conflict with good curving performance in conventional design processes. This conflict problem can be solved with an active steering bogie since active elements properly control the wheelset motions according to track conditions such as straight or curved lines. In this paper, an active steering mechanism for railway vehicle is introduced, and the curving performance of the proposed active steering bogie is investigated through simulation and experiments. According to the results, the proposed active steering bogie is highly effective for curve negotiation.

Keywords: Active steering; Bogie; Railway; Railway vehicle

1. Introduction

A conventional wheelset for railway vehicle is composed of two profiled wheels fixed to a common axle. This wheelset has an advantage of natural curving; however, it has also an unstable mode referred to as "hunting." Hunting phenomenon is a kinematic oscillation of a wheelset on lateral and yawing directions [1]. When a wheelset is unconstrained, hunting is generated even at a very low speed. On a conventional railway vehicle, the wheelset is stabilized by using high stiffness elements connected to the bogie of the vehicle. However, these stiffness elements are known to adversely affect the natural curving of wheelset.

For many years, several researchers have tried to solve the difficult design trade-off between running stability and curving performance using the steering bogie. One commercialized steering bogie is a forced steering bogie [2, 3]. The steering mechanism of the forced steering bogie is composed of mechanical elements such as links and joints. Basic steering principle of the forced steering bogie is the transformation of the relative angular displacement between a car body and a bogie (or between a bogie and a wheelset) in curved track into a steering force and transmitted to a wheelset by links and joints. Curving performance is increased when a forced steering bogie is used. However, it has limitations because of the absence of an active element in the forced steering bogie [4].

The use of active control concepts can overcome the limitations of the forced steering bogie and solve the design conflict between the stability and the steering performance [5, 6]. Likewise, researchers have developed active steering bogies. Schneider and Himmelstein [7] developed an active steering bogie, called "Mechatronic Bogie" or "Flexx Tronic Bogie," which was applied to Swedish Regina 250 train. The bogie's performance has been verified through various field tests toward commercialization. Matsumoto et al. [8] proposed an active-bogie-steering bogie and investigated the curving performance with rolling test stand. The concept is to steer a bogie by actuators against a car body, rather than wheelsets. Anti-yaw dampers between a car body and a bogie are replaced by actuators in this system.

However, the steering mechanism of the Mechatronic Bogie is not suited for urban railway vehicles because it has been developed to control the stability and active steering of high-speed trains with tilting mechanisms. Similarly, the active-bogie-steering bogie, although proposed for urban railway vehicles, has a mechanism that is not applicable to Korean urban railway vehicles because there are no anti-yaw dampers in Korean urban railway vehicles. Therefore, the car body and the bogie should be redesigned so that the active-bogie-steering idea can be adopted.

In this study, an active steering bogie for urban railway vehicles is proposed. Steering mechanism of the proposed bogie controls the wheelset motion when it travels in a curved track. In a straight line, controller is turned-off and wheelsets are

† This paper was recommended for publication in revised form by Associate Editor Hong Hee Yoo

*Corresponding author. Tel.: +82 31 460 5276, Fax.: +82 31 460 5299
E-mail address: jhpark74@krri.re.kr

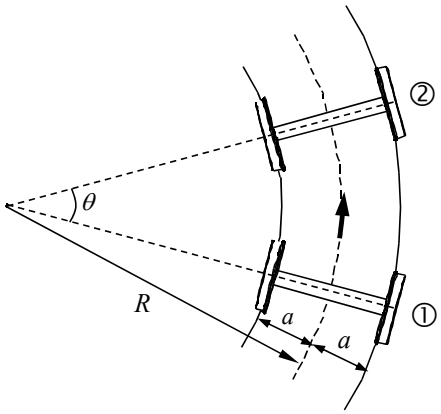

Fig. 1. Curving of a single wheelset.

supported only by the passive suspension elements. Thus, the dynamic characteristic of the proposed bogie is equivalent to the conventional urban vehicle bogie in a straight line. It has the advantage of fail-safe ability because it's stability level without any active elements is similar to that of a conventional urban vehicle. Since the active steering mechanism of the proposed bogie is constructed in the bogie system, a car body of a conventional urban railway vehicle can be used without modification.

The proposed steering mechanism and its kinematic characteristics are described in Chapter 2. Design strategy for the steering mechanism is also introduced in Chapter 2. To estimate the performance of the proposed active steering bogie, simulation results are detailed in Chapter 3, and experiment results using 1/5-scale vehicle are presented in Chapter 4. Finally, Chapter 5 discusses the main conclusions and suggestions for future research.

2. Design of active steering mechanism

2.1 Design strategy of active steering mechanism

The main target of the steering mechanism of railway vehicle is to reduce noise and wear during curve negotiation by steering wheelsets. The noise and wear in curved track are mostly related to longitudinal and lateral creepages of wheelset. The longitudinal and lateral creepages of railway vehicle wheelsets are determined as [9]

$$\xi_x = \frac{\left(\dot{\mathbf{r}}_P^w - \dot{\mathbf{r}}_P^r\right)\cdot \mathbf{t}_1^r}{V}, \tag{1}$$

$$\xi_y = \frac{\left(\dot{\mathbf{r}}_P^w - \dot{\mathbf{r}}_P^r\right)\cdot \mathbf{t}_2^r}{V}, \tag{2}$$

$$\xi_{sp} = \frac{\left(\boldsymbol{\omega}^w - \boldsymbol{\omega}^r\right)\cdot \mathbf{n}^r}{V}, \tag{3}$$

where ξ_x, ξ_y, and ξ_{sp} are longitudinal, lateral, and spin creepages, respectively; $\dot{\mathbf{r}}_P^w$ and $\dot{\mathbf{r}}_P^r$ are the time derivatives for the contact point position vector of wheel and rail in generalized coordinates, respectively; $\mathbf{t}_1^r$ and $\mathbf{t}_2^r$ are the unit orthogonal tangent vectors to the rail at the contact point in the longitudinal and lateral directions; $\mathbf{n}^r$ is the normal vector unit to the surface at the contact point; and V is the magnitude of the wheel velocity along the longitudinal tangent vector at the contact point. The creepages generate the creep forces and creep moments. Generally, large creepages make large creep forces and moments. These creepages, creep forces, and moments are the main factors that affect the wear and noise in curve negotiation.

Fig. 1 shows the curving motion of a single wheelset. Traveling speed of the outer wheel should be faster than that of the inner wheel in order for all the wheels to satisfy pure rolling condition along a curved track. If a wheelset moves from initial position ① to ②, and traveling speed of outer and inner wheels are V_2 and V_1 respectively, V_2 should satisfy Eq. (4),

$$V_2 = \frac{R+a}{R-a}V_1, \tag{4}$$

where R is the radius of the centerline for curved track and a is one-half the gage of the track. Since the conventional wheelset is composed of two wheels fixed to a common axle, as mentioned in Chapter 1, angular speeds of the inner and the outer wheels are equal. Thus, to satisfy Eq. (4), the outer wheel should have a larger rolling radius than the inner wheel. The desired rolling radius difference between the outer and the inner wheels on the curved track whose radius is R can be expressed as,

$$r_{out} = \frac{R+a}{R-a}r_{in}. \tag{5}$$

If the variation of the wheel rolling radius can be expressed using the lateral displacement of a wheel. The desired lateral displacement that can satisfy Eq. (4) or (5) can also be determined as

$$y = \frac{2ar_0}{R\left(\lambda_{inner}+\lambda_{outer}\right)+a\left(\lambda_{inner}-\lambda_{outer}\right)}, \tag{6}$$

where r_0 is the nominal rolling radius of the wheels. λ_{inner} and λ_{outer} are the equivalent conicities of the inner and outer wheels, respectively which have various values according to the lateral displacement of the wheelset. If the profiles of the inner and outer wheels are the same type of perfect cone, λ_{inner} and λ_{outer} have the same constant value independent of lateral displacement of the wheelset. In this case, Eq. (6) can be simplified as,

$$y = \frac{ar_0}{\lambda R}. \tag{7}$$

It should be noted that the lateral displacements of Eqs. (6) and (7) are measured from the centerline of the track. If the lateral position of the wheelset satisfies Eq. (6) or (7), the

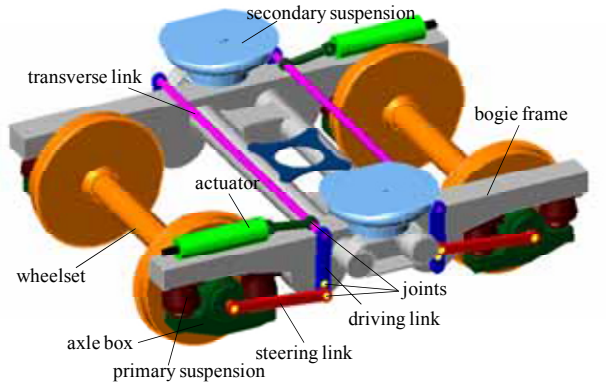

Fig. 2. Design concept of the proposed active steering bogie.

wheelset is in pure rolling condition, and the longitudinal creepages and longitudinal creep forces of the two wheels are ideally zero. Therefore, the wear can be minimized [10].

There are two possible solutions to locate the wheelset to the desired lateral position. One option is to apply a controlled torque to the wheelset in the yaw direction. The lateral and yaw motions of wheelset are dynamically and kinematically coupled. Thus, the lateral motion of wheelset can be controlled by means of controlling yaw motion of the wheelset. Actuators required to generate the yaw torque need to be mounted at the bogie or at the car body. The other option is to install the actuators onto a wheelset in the lateral direction. These actuators also need to be mounted at the bogie or car body. The performances of the two methods are similar. However, the latter method has a drawback: the actuation force controlling the wheelset also act directly on the bogie or the car body in the lateral direction and cause the ride quality to deteriorate [11]. This undesirable effect is expected to be much smaller if the actuators are mounted at the bogie, since the secondary suspensions between the bogie and the car body reduce the vibration. However, yaw control of the wheelset is more practical considering space limitation, ride quality, and so on. Therefore, one of the design strategies of the active steering mechanism is to control the lateral position of wheelset by the yaw directional steering mechanism.

Since railway vehicles in a curved track undergo the centrifugal force, superelevation is constructed in the outer rail to reduce the centrifugal force. However, due to the ride quality and stability problem, superelevation angle is designed to be slightly lower than the balanced angle where the centrifugal force is canceled by the superelevation. As a result, wheelsets move to the outside excessively in a curved track. If the vehicle speed is slower than the regulation speed, wheelsets move inward due to the superelevation. Moreover, the effects of the external forces such as the centrifugal forces, the forces created by the superelevation, and the contact forces produced by the track irregularities change instantaneously; thus, they are different according to each wheelset condition. Therefore, each wheelset should be controlled independently to maximize the active steering performance. This is another design strategy in relation to the active steering mechanism. A control

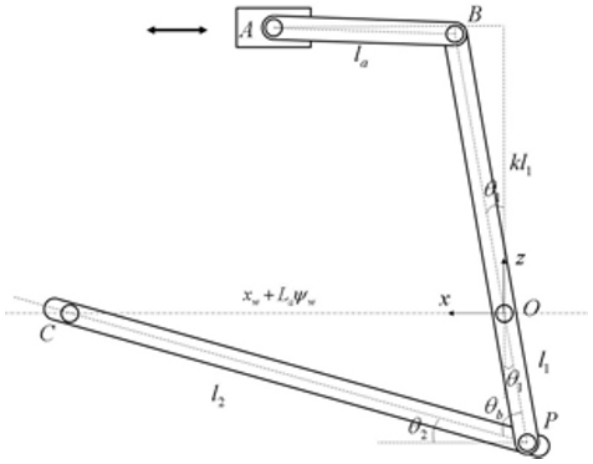

Fig. 3. Kinematic diagram of the proposed steering mechanism.

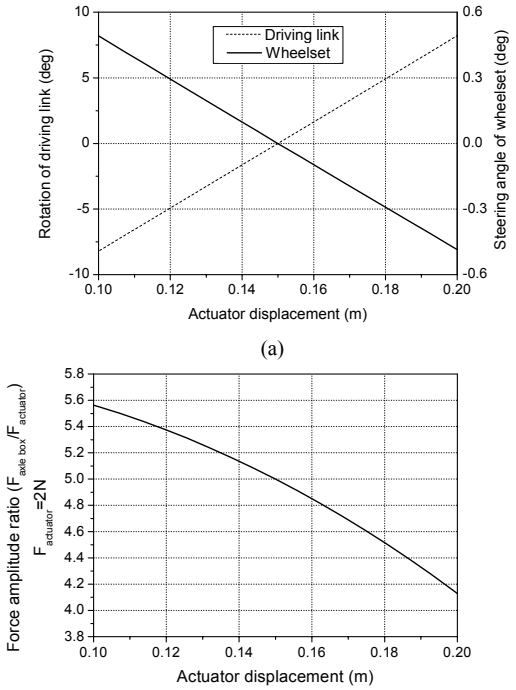

Fig. 4. Kinematic analysis results of the steering mechanism: (a) angular displacements of the driving link and the wheelset with various actuator displacements and (b) force amplitude ratio along the actuator displacement.

strategy for the control of the relative angle between two wheelsets using one controller has been proposed [10]. This method is useful in the steady-state curving condition when all the instantaneous radii of the curved track under each wheelset are equal.

The basic design strategies of the active steering mechanism are summarized as follows:

(1) Control of the lateral displacement of the wheelset,

(2) Control of the lateral displacement of the wheelset by the controlled yaw torque, and

(3) Independent control of each wheelset.

2.2 Active steering bogie

The proposed active steering mechanism is composed of several links and a linear actuator. Fig. 2 shows the schematic design of the active steering bogie in which the proposed active steering mechanisms are implemented. Bogie system of Fig. 2 is a typical Korean urban EMU bogie. In the figure, the proposed steering mechanism can be applied with minimal changes in the main structures and functions of the bogie system. Since, in addition to the active elements, passive primary suspension elements also support the wheelset to the lateral and longitudinal directions, the stability level of the proposed active steering bogie is very similar to the passive bogie.

The proposed active steering mechanism is composed of two driving links, two steering links, a transverse link, and a linear actuator. The driving links are connected to each other through the transverse link and are located on both sides of the bogie frame. Since the driving links are supported to the bogie frame by revolute joints, they can rotate according to the linear motion of the actuator. The steering links are connected between the axle boxes and the driving links by universal joints. Therefore, they can push or pull the axle boxes along with the rotation of the driving links. The positions where the steering links are connected to the driving links are different between left and right sides. For example, the left steering link of the front wheelset is connected to the end of the left driving link but the right steering link is coupled to the middle of the right driving link. Thus, if the actuator pushes the driving links, the left steering link of the front wheelset pushes the left axle box but the right steering link pulls the right axle box. As the result, yawing of the wheelset can be generated. Role of the transverse link is to transmit the displacement and the force of the actuator to the driving links and to synchronize the rotational motions of the left and the right driving links. The active steering mechanisms of the front and rear wheelsets are symmetrically diagonal.

2.3 Kinematic analysis of the steering mechanism

Fig. 3 shows the kinematic diagram of the steering mechanism. *A* is the mover of the linear actuator, *C* is the universal joint between the steering link and the axle box, *O* is the revolute joint between the driving link and the bogie side frame, and *P* is the universal joint between the driving and steering links. Since the yaw motion of the wheelset is small, the kinematic design and analysis of the steering mechanism can be carried out in two-dimensional space. If the steering mechanism does not affect the vertical motion of the wheelset, the point *C* always lies on the *x*-axis. Initial position of C is $(x_w,0)$. If the angular displacement of the driving link is θ_1 due to the linear motion of the actuator mover, the position of the point *C*, namely the axle box becomes $(x_w + L_a\psi_w,0)$, where L_a is the distance between mass center of the wheelset and point *C*. ψ_w is the yaw angle of the wheelset generated by the steering mechanism. From the trigonometric formula, $x_w + L_a\psi_w$ can be calculated as

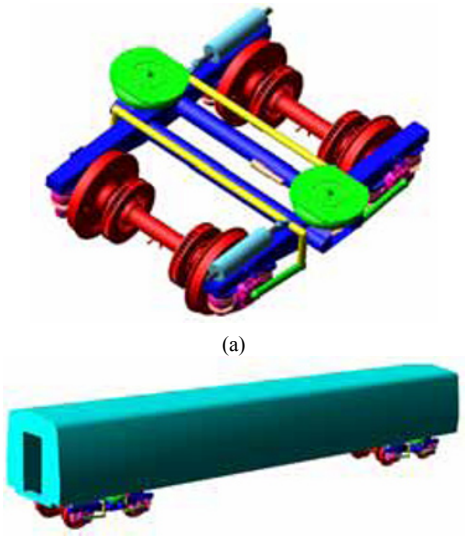

(a)

(b)

Fig. 5. VI-Rail model for numerical simulation: (a) active steering bogie model and (b) full vehicle model.

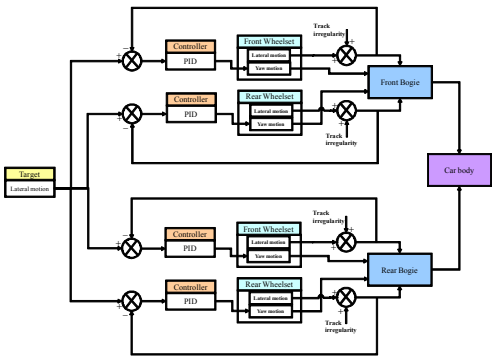

Fig. 6. Control block diagram.

$$x_w + L_a\psi_w = -l_1 \sin\theta_1 + \sqrt{l_2^2 - l_1^2 \cos^2\theta_1} \,. \tag{8}$$

From Eq. (8), steering angle of the wheelset according to the angular displacement of the driving link is expressed as

$$\psi_w = \frac{-l_1 \sin\theta_1 + \sqrt{l_2^2 - l_1^2 \cos^2\theta_1} - \sqrt{l_2^2 - l_1^2}}{L_a} \,. \tag{9}$$

If the design parameters are l_1 and l_2, they should satisfy the following inequality for the maximum steering angle:

$$\psi_{w,\max} \le \frac{-l_1 \sin\theta_1 + \sqrt{l_2^2 - l_1^2 \cos^2\theta_1} - \sqrt{l_2^2 - l_1^2}}{L_a} \,. \tag{10}$$

As shown in Fig. 3, total length of the driving link is $l_1 + kl_1$, and k is the length ratio of *OB* to *OP*. The angular displacements of *OB* and *OP* are equal; however, due to the leverage principle, the moving distance of *B* is k times longer than that of *P*, and the force on *P* is k times larger than on *B*.

The position of *B* from the origin *O* can be expressed using

Table 1. Specifications of the urban railway vehicle for simulation.

Parameters		Values
Mass	Wheelset	1400 (kg)
	Bogie	3800 (kg)
	Car body	28000 (kg)
Moment of Inertia	Wheelset (roll, pitch, yaw)	134, 965, 965 (kg·m^2)
	Bogie (roll, pitch, yaw)	1900,1900,3800 (kg·m^2)
	Car body (roll, pitch, yaw)	90000,38000,90000 (kg·m^2)
Dimension	Axle length	1.97 (m)
	Wheel base (in a same bogie)	2.1 (m)
	Nominal radius of wheel	0.43 (m)
	Wheel conicity	
	Conventional bogie	0.05
	Active steering bogie	0.2
	Distance between bogies	13.8 (m)
Steering mechanism	Driving link	0.42 (m)
	Steering link	0.654 (m)
	Actuator link	0.15 (m)
Stiffness	1st suspension (longitudinal, lateral, vertical)	6.6, 4.4, 1.5 (MN/m)
	2nd suspension (air spring) (longitudinal, lateral, vertical)	0.167, 0.167, 0.37 (MN/m)
Damping	1st suspension (longitudinal, lateral, vertical)	0, 0, 0 (MN·s/m)
	2nd suspension (longitudinal, lateral, vertical)	0, 0.096,0.16 (MN·s/m)
Track	Track gage	1.435 (m)
	Radius of curve (clockwise)	300 (m)
	Cant	152 (mm)

kl_1 and θ_1 as follows:

$$(x_B, z_B) = (kl_1 \sin\theta_1, kl_1 \cos\theta_1). \quad (11)$$

Since the motion of the actuator mover is only the linear reciprocating motion, the vertical position of A is always kl_1. If the actuator mover moves to x_a from the initial position when the driving link revolves from zero to θ_1, position of A is (x_a, kl_1). Since the points A and B are connected by a link whose length is l_a, the distance between A and B has to be equal to l_a and the relation between x_a and l_a is calculated as

$$x_a = kl_1 \sin\theta_1 + \sqrt{l_a^2 - (kl_1 - kl_1 \cos\theta_1)^2}. \quad (12)$$

From Eq. (12), the following inequality can be found:

$$x_a^2 \le (l_a + kl_1)^2 - k^2 l_1^2. \quad (13)$$

A constraint condition of the actuator mover motion can be determined using Eq. (13) when the total length of the driving link and l_a are fixed. From Eq. (12), a constraint for l_a is given as follows:

$$l_a^2 \ge (kl_1 - kl_1 \cos\theta_1)^2. \quad (14)$$

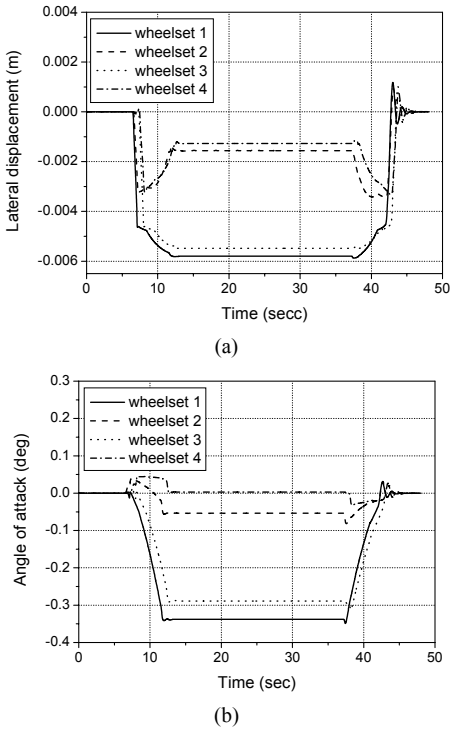

Fig. 7. Wheelset displacements of the conventional vehicle: (a) lateral displacements and (b) angles of attack.

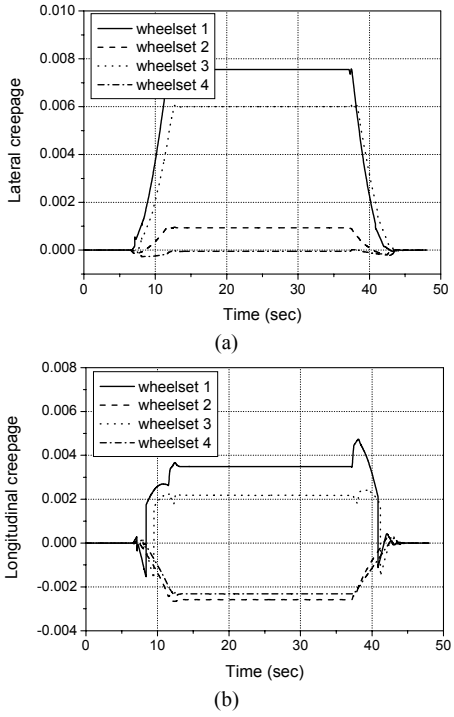

Fig. 8. Creepages of outer wheels for conventional vehicle: (a) lateral creepages and (b) longitudinal creepages.

The design process of the steering mechanism comprises the selection of desired range of the steering angle of the wheelset by the analysis of the track condition. Using Eq. (10), lengths of the driving link and the steering link, and maximum

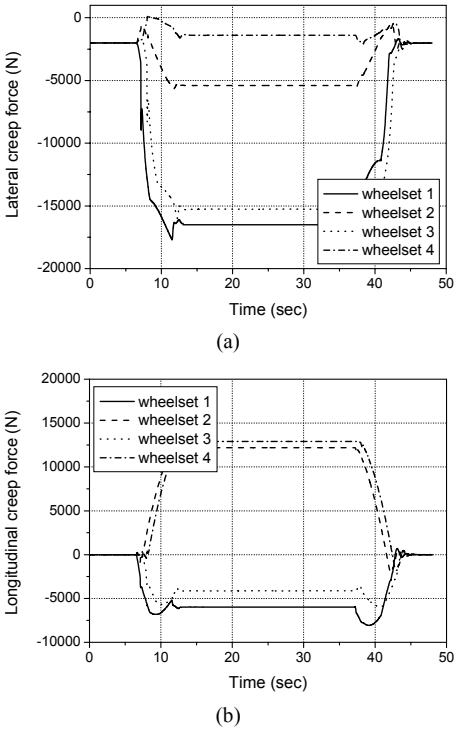

Fig. 9. Creep forces of outer wheels for conventional vehicle: (a) lateral creep forces and (b) longitudinal creep forces.

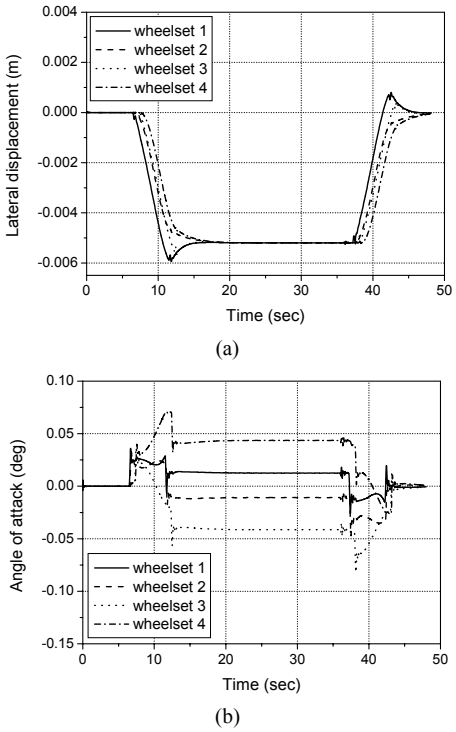

Fig. 10. Wheelset displacements of the proposed active steering bogies: (a) lateral displacements and (b) angles of attack.

angular displacement of the driving link are designed with consideration to space limits and interference problems between the steering mechanism and other existing components. From Eq. (14), proper l_a is selected. From Eq. (13), actuator position and moving range of the actuator mover are calculated.

Disregarding the inertial effects of the links, the steering force of each axle box can be expressed as Eq. (15) when the actuator force is F_a.

$$F_{wx} = \left(X_1 \sin\theta_1 + X_2 \sin\theta_1 + X_3 \cos\theta_1 - X_4 \cos\theta_1\right) \cdot \left(\pm \frac{1}{2} F_a\right), \quad (15)$$

$$X_1 = \frac{\left(x_a - kl_1 \sin\theta_1\right)\left(x_a^2 - l_a^2\right)}{2kl_1 l_a^2}, \quad (16)$$

$$X_2 = \frac{\left(kl_1 - kl_1 \cos\theta_1\right)\left(l_a^2 - x_a^2 + 2kl_1 l_a\right)}{2kl_1 l_a^2}, \quad (17)$$

$$X_3 = \frac{\left(x_a - kl_1 \sin\theta_1\right)\left(l_a^2 - x_a^2 + 2kl_1 l_a\right)}{2l_1 l_a^2}, \quad (18)$$

$$X_4 = \frac{\left(kl_1 - kl_1 \cos\theta_1\right)\left(x_a^2 - l_a^2\right)}{2l_1 l_a^2}. \quad (19)$$

Since the actuation force is divided into two and transmitted to the left and the right driving links by the transverse link, the upper sign in Eq. (15) is for the right axle box. The lower is for the left axle box.

Fig. 4 shows an example of the kinematic analysis results when l_1 is 0.07 m, l_2 is 0.654 m, and l_a is 0.15 m. Leverage ratio (k) is 5. In Fig. 4 (a), steering angle of the wheelset has a linear relation to the actuator stroke. It is also linear to the angular displacement of the driving link. However, force amplitude ratio is not linear to the actuator stroke because the direction of the actuator force exerted on the driving link is changed according to the actuator stroke. Generally, desired steering angle is less than 0.3^o in most curved tracks, the maximum stroke of the actuator will be about ±0.03 m from the nominal position and the force amplitude ratio will be approximately 5.4-4.5.

3. Simulation

To estimate the performance of the proposed active steering mechanism, and to evaluate steering effects, numerical simulation was carried out. VI-Rail, one of the famous commercial S/W for dynamic analysis of railway vehicles, is used for the simulation. Fig. 5 shows the VI-Rail model for simulation and main parameter values are given in Table I.

In order to simplify control algorithm, wheel profile of the active steering bogie is selected as a cone type with linear conicity 0.2. Even though a linear cone type profile is not suitable for real railway vehicle, it is appropriate for analyzing the performance of steering mechanism because the nonlinear effects generated by nonlinear wheel profile can be disregarded. To implement the active steering bogie to a real railway vehicle, the wheel profile has to be modified but the

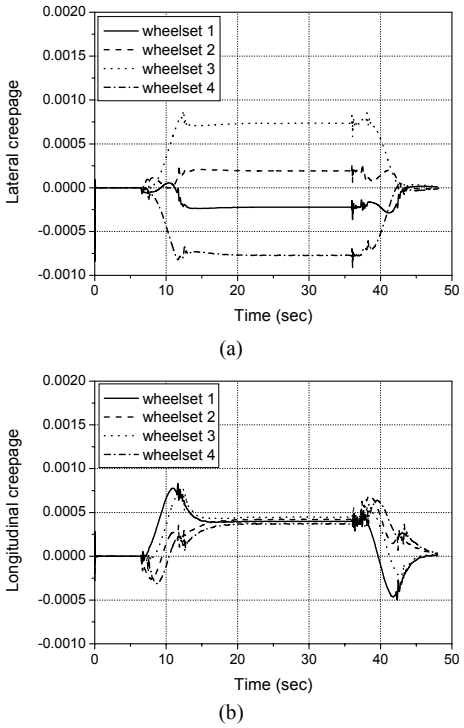

Fig. 11. Creepages of outer wheels for the proposed active steering bogie: (a) lateral creepages and (b) longitudinal creepages.

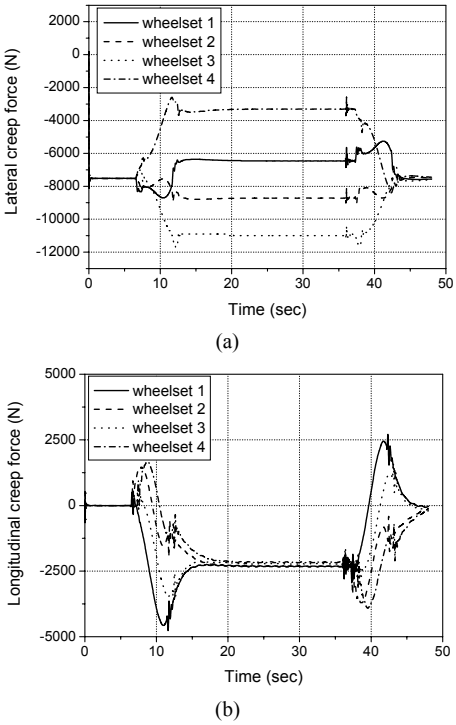

Fig. 12. Creep forces of outer wheels for the proposed active steering bogies: (a) lateral creep forces and (b) longitudinal creep forces.

equivalent conicity will be maintained at 0.2.

In the simulation, four PID controllers are used to control the lateral displacement of each wheelset. Control block diagram is shown in Fig. 6. As mentioned in Chapter 2, control forces are exerted on the yaw direction of the wheelsets.

In a railway vehicle, frequency range for a wheelset negotiating an arbitrarily curve is generally less than 1 Hz. This implies that bandwidth of the active steering mechanism should be 1 Hz or higher. In this work, bandwidth of the active mechanism was selected as 3 Hz. In order to achieve an actuator force range, the maximum steering angle was calculated, 0.3° at 3 Hz. Control gains for the generated control forces are tuned to be within the calculated actuator force range, to satisfy the servo bandwidth (3 Hz). Selected gains are 1×10^7, 2×10^6, and 4.3×10^6 for P, I, and D.

Fig. 7 shows the lateral displacements and the angles of attack for each wheelset in a conventional vehicle. All data are calculated from the reference coordinates on the track centerline. Positive x-axis of the reference frame is the running direction of the vehicle and positive z-axis is the gravitational direction. Wheelsets 1 and 2 denote front and rear wheelsets of front bogie and Wheelsets 3 and 4 indicate front and rear wheelsets of rear bogie, respectively. In Fig. 7(a), all the wheelsets move to outer rail due to the centrifugal force. Specifically, flange contact is generated on the front wheelsets of all bogies. Lateral displacements of rear wheelsets are relatively small compared to the front wheelsets because of the yaw displacements of bogies. Angles of attack of front wheelsets are also larger than those of rear wheelsets.

Fig. 8 displays the lateral and the longitudinal creepages of outer wheels. Fig. 9 shows the creep forces. From the simulation results, curving performance of the front wheelset is estimated to be very poor. Large creepages and creep forces give rise to severe wear of wheel and rail. Particularly, large lateral creepages and creep forces generated by the flange contact cause flange wear and flange squeal noise. In addition, large longitudinal creepages and creep forces are two of the dominant factors for wheel tread wear. Therefore, steering performance should be enhanced in conventional urban vehicles.

Fig. 10 shows the lateral displacements and the angles of attack of wheelsets when the proposed active steering bogies are applied. Track condition is the same with the former simulation. In Fig. 10(a), wheelsets were controlled well to track the desired lateral displacement calculated as 5.13 mm from Eq. (7). The angles of attack of Wheelsets 1 and 3 are reduced remarkably, but somewhat increased in the case of Wheelsets 2 and 4.

The lateral and the longitudinal creepages of outer wheels are decreased outstandingly, as shown in Fig. 11. Lateral creep forces are also decreased in a curved line (7-43 s) but are increased in a straight line in Fig. 12(a), compared to Fig. 9(b). Spin creepages affect the lateral creep forces and large spin creepage produces large lateral creep force. Since the spin creepage increases with the conicity, the lateral creep forces of the proposed bogie in straight line are larger than those of the conventional bogie. However, the variation of lateral creep force between the straight line and the curved line is small in the proposed bogie. Fig. 12(b) shows that longitudinal creep

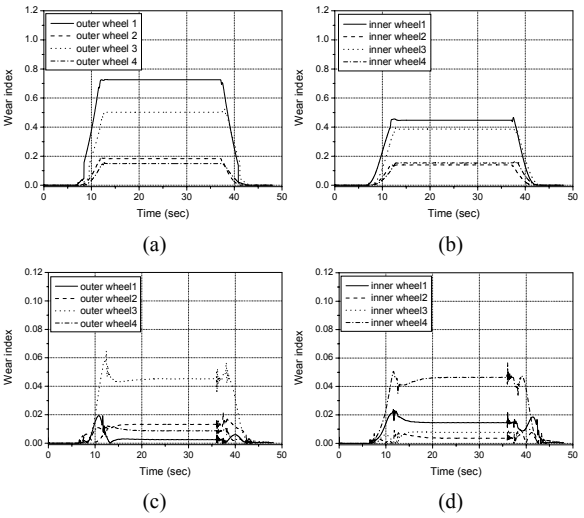

Fig. 13. Wear indices of conventional and active steering vehicles: (a) outer wheels and (b) inner wheels of conventional vehicle; (c) outer wheels and (d) inner wheels of active steering vehicle.

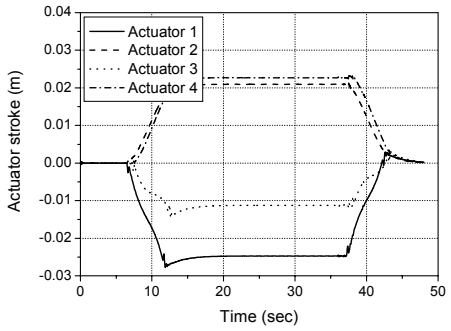

Fig. 14. Strokes of each actuator during control process.

forces can be reduced when the wheelsets are controlled actively.

One of the useful parameters to describe the enhancement of curving performance due to active steering control is wear index [12]. Wear index below 0.8 is considered as "low wear" and above 0.8 as "high wear" [11]. Wear index is defined as Eq. (20):

$$W = \begin{cases} 0.005 \cdot \left(F_x \cdot \xi_x + F_y \cdot \xi_y\right), \left(F_x \cdot \xi_x + F_y \cdot \xi_y\right) \le 160\text{N} \\ 0.025 \cdot \left(F_x \cdot \xi_x + F_y \cdot \xi_y\right) - 3.2 \end{cases} . \quad (20)$$

Fig. 13 demonstrates the wear index of the conventional and active steering vehicles on curved track. Maximum wear index of the conventional vehicle is 0.72 at front outer wheel of front bogie and the minimum at rear inner wheel of rear bogie is 0.14. In the case of the active steering vehicle, maximum is 0.065 at front outer wheel of rear bogie and minimum is 0.0026 at front outer wheel of front bogie. Simulation results show that active steering can reduce the wear index above 80% and can be more powerful on tight curves.

In the active steering process, Actuator 1 has the maximum stroke among the four actuators and Actuator 3 has the minimum. In Fig. 14, Actuators 1 and 2 indicate front and rear actuators of the front bogie, respectively, and Actuators 3 are 4 for rear bogie.

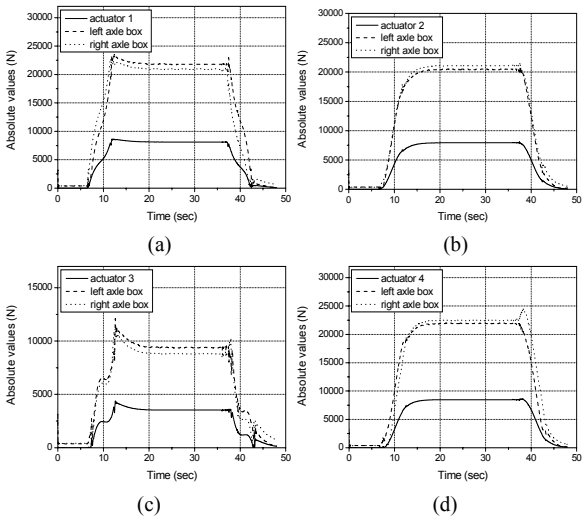

Fig. 15. Absolute values of the control force and the steering force: (a) front wheelset and (b) rear wheelset of the front bogie; (c) front wheelset and (d) rear wheelset of the rear bogie.

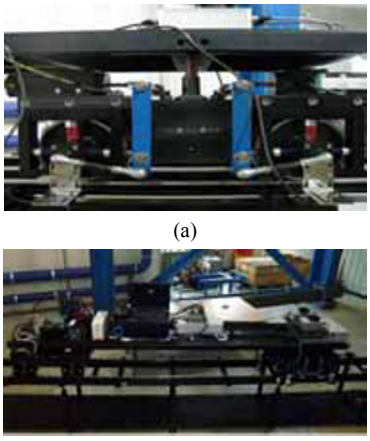

Fig. 16. Scaled vehicle model: (a) scaled active steering bogie and (b) scaled full vehicle.

Fig. 15 shows absolute values of the control forces from the actuators and the steering forces exerted on each axle box. As predicted in Chapter 2, the steering forces are about five times larger than the half of actuator forces.

4. Experiment with 1/5-scale vehicle

A 1/5-scale vehicle is constructed to verify the performance of the proposed active steering mechanism. Tests and experiments in the railway vehicle research have widely used the scaled railway vehicle because of a large cost saving, ease of operability, and ease of changing a large number of vehicle parameters even with the presence of scaling errors in contact mechanics. It is very useful to compare the steering performance between the active steering bogie and the passive bogie.

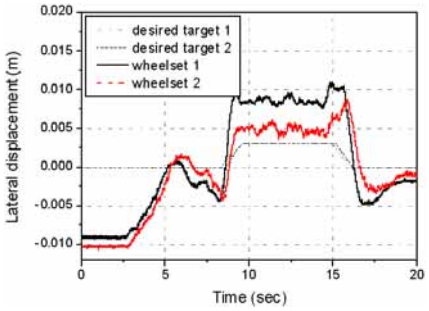

Fig. 17. Lateral displacements of the steering bogie wheelsets without control.

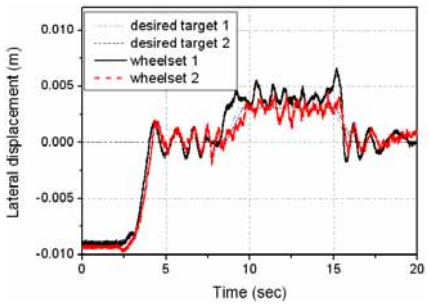

Fig. 18. Lateral displacements of the steering bogie wheelsets with active control.

Fig. 16 shows a 1/5-scale active steering bogie and a scaled vehicle. Due to space problem, electromagnetic linear actuators are located at the middle of the bogie. Leverage ratio of the driving link is 5 and spherical joints are used instead of universal joints. Combinations of coil springs are used to match the scaling law for the stiffness of the suspensions. The scaled bogie is manufactured according to Iwnicki's scaling law [13]. The scaled vehicle is composed of a traction bogie, an active steering bogie, and a car body. Controllers using dSPACE 1103 control the vehicle speed and the lateral displacements of each wheelset. Lateral displacements of the wheelsets are measured with four laser displacement sensors.

Track and rail profile are also scaled along the scaling law. Total length of the scaled track is 27 m. The straight line for acceleration is 6.5 m, curved line of 20 m radius is 14 m, and the other straight line for deceleration is 6.5 m. In the middle of curved rail, strain gages are attached to measure the deformation of the rails when the vehicle is passing.

Fig. 17 shows the lateral displacement of the wheelsets without control. The scaled vehicle starts to move at 3 s and accelerates until the speed becomes 2 m/s. Initial positions of wheelsets were approximately -10 mm from the center of the track; however, when the vehicle starts to travel, the lateral displacements converge to zero due to the creep forces. On curved line, wheelsets move to the outside of the rail because of the centrifugal force and the front wheelset undergoes the flange contact.

Fig. 18 illustrates the controlled lateral displacements of wheelsets using fuzzy control algorithm. Wheelsets track the desired lateral displacement well, even though there are some

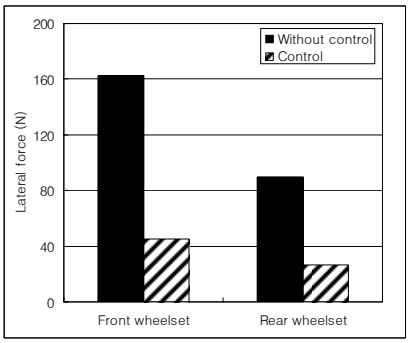

Fig. 19. Comparison of lateral forces exerted on wheelsets.

tracking errors and vibrations. It is expected that the error and the vibration can be reduced through fine-tuning the control gains.

Lateral forces exerted on the wheelsets by the reaction of the rails can be acquired using the measured data from the strain gages on the rails. In Fig. 19, active steering control reduces the lateral forces by about 70%.

5. Conclusion

In this paper, an active steering bogie is proposed for urban railway vehicles. Secondly, active steering mechanism using leverage principle is suggested. Due to the leverage principle, the proposed steering mechanism has the advantage of control over the wheelsets using low control forces. Since wheelsets are constrained by high stiffness primary suspensions required to acquire high running stability, active steering force should be sufficiently large to overcome the high stiffness force of primary suspension; however, it is difficult to use high power actuator because of cost, space, and weight problems. The easiest way is to use soft primary suspension or eliminate the longitudinal and lateral stiffness of the primary suspension. In this case, active mechanism has to play a role of stabilizer for the wheelset and steering. Furthermore, additional fail-safe function should be developed against emergencies such as control failure and sensor trouble.

In the proposed active steering bogie, high stiffness primary suspensions stabilize the wheelset on high-speed straight line, and the proposed active mechanisms control the steering on low-speed curved line. The active mechanism is turned off when an emergency occurs. Then, the proposed bogie becomes a passive bogie with high stability and low steering performance. To cope with the high primary suspension force, lever ratio was selected to be 5.

Kinematic design and analysis for the proposed steering mechanism were carried out mathematically, and the performance is verified with dynamic simulation using VI-Rail and several experiments. From the simulation, the proposed active steering bogie is proven to have high curve negotiation performance. The creepages and creep forces, which are dominant factors that cause squeal noise and wheel/rail wear, were significantly reduced. Steering performance of the proposed bogie is also estimated by experimental investigation using a 1/5-scale mod-

el. The proposed bogie is found to be practical and the steering mechanism is feasible for urban railway vehicle.

In future studies, more useful control strategy to satisfy pure rolling condition will be developed and proper wheel profile designed instead of the perfect cone type. Optimal stiffness of primary suspension will be also studied in order to reduce the control force and to maintain the minimum stability criteria.

References

[1] S. Iwnicki,, *Handbook of Railway Vehicle Dynamics*, CRC Press, Boca Raton, USA, (2006).

[2] T. Suga, *Japanese Railway Technology Today*, East Japan Railway Culture Foundation, Japan, (2001) 19-34.

[3] R. E. Smith, Performance Testing of the Resco Steered Frame Freight Car Truck at the AAR Test and Comparisons with Standard and Premium Three-Piece Trucks, *Resco engineering Project Report*.

[4] J. H. Park, H. M. Hur, H. I. Koh and, W. H. You, Concept Design of an Active Steering Bogie for Urban Railway Vehicles, *J. the Korean Society for Railway (Korean)*, 10 (6) (2007) 709-716.

[5] T. X. Mei and R. M. Goodall, Wheelset control strategies for a 2-axle railway vehicle, *J. Vehicle system Dynamics*, 33 (2000) 653-664.

[6] J. T. Pearson, R. M. Goodall, T. X. Mei and G. Himmelstein, Active stability control strategies for a high speed bogie, *Control Engineering Practice, Elsevier*, 12 (2004) 1381-1391.

[7] R. Schneider and G. Himmelstein, Active Radial Steering and Stability Control with the Mechatronic Bogie, *WCRR conference* (2006).

[8] A. Matsumoto, Y. Sato, H. Ohno, Y. Suda, Y. Michitsuji, M. Komiyama, M. Tanimoto, Y. Kishimoto, Y. Sato and T. Nakai, Multibody Dynamics Simulation and Experimental Evaluation for Active-Bogie-Steering Bogie, *Proc. Int'l Symposium on Speed-up and Service Technology for Railway and Maglev Systems*, (2005) 103-107.

[9] A. A. Shabana, K. E. Zaazaa and H. Sugiyama, *Railroad Vehicle Dynamics: A Computational Approach*, CRC Press, New York, USA, (2008) 140-142.

[10] J. Pérez, J. M. Busturia and R. M. Goodall, Control Strategies for Active Steering of Bogie-Based Railway Vehicles, *Control Engineering Practice, Elsevier*, 10 (2002) 1005-1012.

[11] T. X. Mei, R. M. Goodall, Recent Development in Active Steering of Railway Vehicles, *J. Vehicle System Dynamics*, 39 (6) (2003) 415-436.

[12] F. González, J. Pérez, J. Vinolas and A. Alonso, Use of Active Steering in Railway Bogies to Reduce Rail Corrugation on Curves, *Proc. Instn. Mech. Engrs., Part F: J. Rail and Rapid Transit*, 221 (2007) 509-519.

[13] H. M. Hur, J. H. Park, M. S. Kim, W. H. You and T. W. Park, A Study on the Critical Speed of 1/5 Scaled Bogie Model, *J. the Korean Society for Railway (Korean)*, 10 (6) (2007) 800-805.

Joon-Hyuk Park received his B.S. (KAIST, Daejeon, Korea in 1998), and his M.S. and Ph.D. (Yonsei University, Seoul, Korea in 2000 and 2005, respectively) in Mechanical Engineering. Currently, he is a senior researcher at the Vehicle Dynamics and Propulsion Research Department of Korea Railroad Research Institute. His research interests are related to vehicle dynamics, including the mechatronic railway vehicle, and running test and evaluation technology for railway vehicles.

Hyo-In Koh received her M.A. degree (2001) and her Ph.D. (2004) in Technical Acoustics from the Technical University of Berlin, Germany. She is a senior researcher at the Railway Environment Research Department. Her research interests are related to noise reduction and acoustical environment in the railway system.

Hyun-Moo Hur obtained his B.S. and M.S. in Mechanical Engineering degrees from Yonsei University, Korea, in 1988 and 1990 respectively. He received his Ph.D. from Ajou University, Suwon, Korea in 2009. He is currently a principal researcher in the Korea Railroad Research Institute in Korea. His research interests include railway vehicle dynamics and wheel/rail interface.

Min-Soo Kim obtained his B.S., M.S., and Ph.D. degrees in Electrical Engineering from Soongsil University, Seoul, Korea in 1995, 1997, and 2003, respectively. From December 2005 up to the present, he is a senior researcher at the Vehicle Dynamics and Propulsion Research Department at Korea Railroad Research Institute. His research interests include control systems design of railway vehicle and dynamometer test for the railway brake components.

Won-Hee You received his M.S. and Ph.D. degrees in Mechanical Engineering from Yonsei University, Seoul, Korea in 1984 and 1993, respectively. He is a chief researcher at the Vehicle Dynamics and Propulsion Research Department in Korea Railroad Research Institute. His research interests are related to vehicle dynamics including the mechatronic railway vehicle and railway noise and vibration.